Hydroxylated furanoditerpenoids from pupal cases produced by the bruchid beetle *Sulcobruchus sauteri* inside the seeds of *Caesalpinia decapetala*

Yui Akihara [a], Sayuri Kamikawa [a], Yui Harauchi [a], Emi Ohta [a], Tatsuo Nehira [b], Hisashi Ômura [a], Shinji Ohta [a,*]

[a] *Graduate School of Biosphere Science, Hiroshima University, 1-7-1 Kagamiyama, Higashi-Hiroshima 739-8521, Japan*

[b] *Graduate School of Integrated Arts and Sciences, Hiroshima University, 1-7-1 Kagamiyama, Higashi-Hiroshima 739-8521, Japan*

* Corresponding author.

E-mail address: ohta@hiroshima-u.ac.jp (S. Ohta)

ABSTRACT

Seven undescribed hydroxylated cassane-type furanoditerpenoids were isolated from pupal cases formed from the secretion/excretion of the larvae of the wild bruchid seed beetle *Sulcobruchus sauteri* in infested *Caesalpinia decapetala* seeds, and their structures were elucidated by interpreting their spectra. The hydroxylated furanoditerpenoids found in the pupal cases were not present in the seeds of the host plant. Caesalacetal and caesaljapin obtained from the intact seeds exhibited larvicidal activity against the larvae of *Aedes albopictus*, while the hydroxylated furanoditerpenoids isolated from the pupal cases were inactive. The larvae of *S. sauteri* are proposed to detoxify larvicidal diterpenoids that occur in the seeds of the host plant by regiospecific hydroxylation.

Keywords: *Caesalpinia decapetala*; Leguminosae; Bruchid seed beetle; *Sulcobruchus sauteri*; cassane diterpenoid; detoxification

1. Introduction

The seeds of *Caesalpinia decapetala* (Roth) Alston (Leguminosae: synonym *Caesalpinia decapetala* var. *japonica*, with the common Japanese name 'jaketsuibara') have been used as an insecticide, an antidiarrheal agent, and a febrifuge for malarial fever in oriental traditional medicine (Namikoshi et al., 1987). The seeds have been reported to contain cassane-type furanoditerpenoids, such as caesaljaponin A (**1**) (Kamikawa et al., 2015). The seed-eating larvae of the wild bruchid beetle *Sulcobruchus sauteri* specifically infest the seeds of *C. decapetala*, feed on their cotyledon, and produce pupal cases (Fig. 1) prior to pupation, using secretion/excretion products inside the seeds (Watanabe, 1985). In the course of our investigations into biologically active compounds involved in the relationship between the seed-eating larvae of the bruchid beetle and its host plant, we isolated seven undescribed hydroxylated furanoditerpenoids from the MeOH extracts of the pupal cases produced by *S. sauteri*. In this paper we report our investigations into the structures and larvicidal activities of the furanoditerpenoids isolated from the intact seeds of *C. decapetala* and the pupal cases produced by the bruchid beetle *S. sauteri*.

2. Results and Discussion

The intact seeds of *C. decapetala* and the pupal cases produced by the larvae of the bruchid beetle *S. sauteri* inside the infested seeds (Fig. 1) were extracted with MeOH. Each of the concentrated MeOH extracts was suspended in water and successively partitioned with hexane and EtOAc. Each EtOAc-soluble portion was subjected to analysis by HPLC with photodiode-array detection (HPLC-PDA) (Fig. 2). The EtOAc-soluble fraction of the intact seeds showed the presence of relatively apolar components (Fig. 2A), which were identified as caesaljaponin A (**1**), caesaljaponin B (**2**) (Kamikawa et al., 2015), caesalacetal (**3**) (Kamikawa et al., 2016a), and caesaljapin (**4**)

(Ogawa et al., 1992; Kamikawa et al., 2016a) based on comparisons of their spectroscopic data with those of authentic samples after isolation by silica gel column chromatography (CC), while HPLC analysis of the EtOAc-soluble portion derived from the pupal cases revealed the presence of several major polar components (Fig. 2B). This portion was subjected to octadecylsilyl (ODS) CC followed by purification by ODS or silica gel CC to afford compounds **5**–**11** (Fig. 3).

Compound **5** was isolated as a colorless oil with an optical rotation, $[\alpha]_D$, of –28˚ (*c* 0.04, MeOH). Positive-ion HRESIFTMS revealed an $[M+Na]^+$ ion peak at *m/z* 413.1570 (calcd for $C_{21}H_{26}O_7Na^+$, 413.1571), consistent with the molecular formula $C_{21}H_{26}O_7$ (nine degrees of unsaturation). IR-absorption bands at 3396, 1760, and 1724 cm^{-1} implied the presence of hydroxyl, γ-lactone, and ester functionalities. The ^1H NMR spectrum exhibited a pair of doublets at δ_H 6.46 (1H, d, J = 1.8 Hz, H-15) and 7.36 (1H, d, J = 1.8 Hz, H-16), indicating the presence of a 1,2-disubstituted furan ring, which was supported by a UV absorption maximum at 216 nm (log ε 4.02) as well as IR absorption bands at 1507 and 1456 cm^{-1} (Jiang et al., 2002; Ochieng et al., 2012; Kamikawa et al., 2015, 2016a, 2016b). The ^{13}C NMR and DEPT spectra, as well as HSQC spectrum, revealed the presence of 21 carbon signals that correspond to three methyl groups (including a methoxy carbon), five methylenes, three methines (including an oxygenated carbon), six quaternary carbons (including two oxygenated carbons), and two carbonyl carbons, in addition to the four sp^2 carbon atoms at δ_C 148.6 (C-12, s), 122.4 (C-13, s), 109.1 (C-15, d), and 143.1 (C-16, d) of the 1,2-disubstituted furan ring. The ^1H–^1H COSY and HSQC spectra established the presence of four partial structures (C-1/C-2/C-3, C-5/C-6/C-7, C-9/C-11, and C-15/C-16), as shown in Fig. 4. The connectivity between C-3 and C-5 through C-4 was determined on the basis of HMBC correlations from H_3-19 to C-3, C-4 and C-5. The connectivities between the remaining partial structures were deduced by analysis of the HMBC spectroscopic data,

which included key correlations from H-1 to C-5, C-10, and C-20, from H-7 to C-8, from H_2-11 to C-8, C-12, and C-13, from H-15 to C-12, from H-16 to C-13, and from H_3-17 to C-8, C-13, and C-14, which resulted in the cassane-type furanoditerpene skeleton in **5** (Fig. 4). The HMBC correlations from H_3-19 and the methoxy protons at δ_H 3.70 (H_3-21) to the carbonyl carbon at δ_C 178.5 (C-18) established that the methoxycarbonyl group is attached to C-4. Since the presence of the furan ring, the A–C rings, and two carbonyl groups account for eight of the nine degrees of unsaturation, compound **5** must have a lactone ring, which is supported by the IR absorption band at 1760 cm^{-1}. The chemical shifts of C-8 (δ_C 88.5) and C-20 (δ_C 180.5) indicated the presence of a γ–lactone moiety bridged between C-8 and C-10. The chemical shifts of H-2/C-2 (δ_H 4.22 and δ_C 63.8) and C-14 (δ_C 70.1) indicated that C-2 and C-14 bear hydroxyl groups. All other HMBC correlations supported the overall structure of **5**, as shown in Fig. 4. The relative configuration of **5** was established by coupling-constant analyses and NOESY data (Fig. 5). NOESY correlations between H-9 and both H-5 and H-7α indicated that these protons were all axial and *α*-oriented. On the other hand, the NOESY correlation between H-2 and Me-19 indicated that the hydroxyl group at C-2 and Me-19 were α- and β-oriented, respectively. The equatorial and α-orientation of 2-OH was supported by the large vicinal coupling constant of 11.9 Hz between H-2 and both H-1α and H-3α. The NOESY correlation between H-7β and Me-17 indicated that Me-17 was β-oriented, which was supported by the other NOESY correlation between H-15 and Me-17. The absolute configuration of **5** was determined by comparison of the experimentally acquired electronic circular dichroism (ECD) spectrum of **5** with that calculated using the time-dependent density functional theory (TDDFT) method. Compound **5** exhibited positive Cotton effects (CEs) at 190 nm (Δε +2.01) and 247 nm (Δε +0.42), and a negative CE at 216 nm (Δε –2.86), which were in good agreement with those calculated for the 2*S*-configured model (Fig. 6). Consequently, the structure

of **5** was established as shown in Fig. 3. The compound was named caesalsauteolide.

Compound **6** was obtained as a colorless oil with an optical rotation, $[\alpha]_D$, of +8˚ (*c* 0.1, MeOH). Negative-ion HRESIFTMS analysis revealed an $[M–H]^-$ ion peak at *m/z* 375.1817 (calcd for $C_{21}H_{27}O_6^-$, 375.1813), consistent with the molecular formula $C_{21}H_{28}O_6$. The NMR spectra of **6** were almost identical to those of caesaljapin (**4**) (Ogawa et al., 1992; Kamikawa et al., 2016a) except for the presence of additional oxygenated methine signals at δ_H 4.19 (m) and δ_C 65.2 (CH), which indicated the presence of a new hydroxyl group. Analyses of the $^1H–^1H$ COSY and HSQC spectra revealed the additional hydroxyl group to be located at C-2 (Fig. 4). The α-orientation of the 2-OH was evidenced by the large $^3J_{H1\alpha\text{-}H2}$ (11.7 Hz) and $^3J_{H2\text{-}H3\alpha}$ (12.2 Hz) coupling constants. All other HMBC and NOESY correlations supported the overall structure and relative configuration of **6**, as shown in Figs. 4 and 5. The ECD spectrum of compound **6** exhibited a positive CE at 216 nm (Δε +2.67), which was similar to that of caesaljapin (**4**) ($\Delta\varepsilon_{218}$ +8.89) (Kamikawa et al., 2016a). As it had been reported that the CE attributed to the π–π* transition of a furan chromophore in such a furanoditerpenoid is mainly affected by the chirality of C-14 (Wu et al., 2014), the absolute configuration at C-14 in **6** was assigned to be *R*. Consequently, the structure of **6** was established as shown in Fig. 3. The compound was named 2-hydroxycaesaljapin.

Compound **7** was obtained as a colorless oil with an optical rotation, $[\alpha]_D$, of +3˚ (*c* 0.2, MeOH). Negative-ion HRESIFTMS revealed an $[M–H]^-$ ion peak at *m/z* 391.1765 (calcd for $C_{21}H_{27}O_7^-$, 391.1762), consistent with the molecular formula $C_{21}H_{28}O_7$, which differs from that of 2-hydroxycaesaljapin (**6**) by one oxygen atom. This difference suggested that compound **7** contains an additional hydroxyl group. The NMR spectra of **7** were almost identical to those of **6** except for the absence of the C-7 methylene signals and the presence of additional oxymethine signals at δ_H 3.51 (td, J = 10.7 and 4.9 Hz) and δ_C 72.3 (CH). The $^1H–^1H$ COSY and HMBC spectra indicated that

compound **7** is a 7-hydroxylated derivative of **6** (Fig. 4). The large ^{1}H coupling constant of 10.7 Hz between H-7 and both H-6β and H-8 is evidence of the equatorial and β-orientation of the 7-OH. All other HMBC and NOESY correlations supported the overall structure and relative configuration of **7**, as shown in Figs. 4 and 5. Compound **7** exhibited a positive CE at 215 nm (Δε +2.60) in its ECD spectrum, which is similar to those of **6** ($\Delta\varepsilon_{216}$ +2.67) and caesaljapin (**4**) ($\Delta\varepsilon_{218}$ +8.89) (Kamikawa et al., 2016a). Therefore, the absolute configuration of C-14 in **7** was determined to be the same as **4** and **6**. Consequently, the structure of **7** was established as shown in Fig. 3. The compound was named 2,7-dihydroxycaesaljapin.

Compound **8** was obtained as a colorless oil with an optical rotation, $[\alpha]_D$, of +19˚ (*c* 0.004, MeOH). Positive-ion HRESIFTMS revealed an $[M+Na]^+$ ion peak at *m/z* 399.1778 (calcd for $C_{21}H_{28}O_6Na^+$, 399.1778), consistent with the molecular formula $C_{21}H_{28}O_6$. The NMR spectra of **8** were almost identical with those of caesalacetal (**3**) (Kamikawa et al., 2016a), except for the presence of additional oxygenated methine signals at δ_H 4.21 and δ_C 65.6. These observations indicated that compound **8** contains an additional hydroxyl group, which is attached to C-2 on the basis of the ^{1}H–^{1}H COSY, HSQC, and HMBC spectra (Fig. 4). The α-orientation of the 2-OH was verified by the large $^{3}J_{H1\alpha\text{-}H2}$ (11.0 Hz) and $^{3}J_{H2\text{-}H3\alpha}$ (12.2 Hz) coupling constants and an NOE correlation between H-2 and Me-19 (Fig. 5). All other HMBC and NOESY correlations supported the overall structure and relative configuration of **8**, as shown in Figs. 4 and 5. Compound **8** exhibited a positive CE at 219 nm (Δε +1.72) in its ECD spectrum, which is associated with the π–π* transition of the furan chromophore, in good agreement with that of caesalacetal (**3**) ($\Delta\varepsilon_{218}$ +5.62) (Kamikawa et al., 2016a). As it had been reported that the CE of **3** is mainly determined by the chirality on C-14 (Wu et al., 2014; Kamikawa et al., 2016a), the absolute configuration at C-14 in **8** was assigned to be *R*. Consequently, the structure of **8** was established as shown in Fig. 3. The compound was

named 2-hydroxycaesalacetal.

Compound **9** was obtained as a colorless oil with an optical rotation, $[\alpha]_D$, of –6˚ (*c* 0.2, MeOH). Positive-ion HRESIFTMS revealed an $[M+Na]^+$ ion peak at *m/z* 399.1779 (calcd for $C_{21}H_{28}O_6Na^+$, 399.1778), consistent with the molecular formula $C_{21}H_{28}O_6$. The NMR spectra were similar to those of caesalpinista A (**12**) (Yang et al., 2009; Kamikawa et al., 2016b), except for the absence of signals for C-2 and C-17, and the presence of signals that correspond to an oxymethine at δ_H 3.81 (m, H-2) and at δ_C 64.4 (C-2), and an exocyclic double bond at δ_H 5.05 (d, J = 2.1 Hz, H-17a), δ_H 4.78 (d, J = 2.1 Hz, H-17b), δ_C 144.2 (C-14), and δ_C 103.7 (C-17). These observations indicated that compound **9** is a $\Delta^{14,17}$-2-hydroxy derivative of caesalpinista A (**12**), which was supported by ^1H–^1H COSY and HMBC spectra (Fig. 4). The α-orientation of the 2-OH was verified by the large $^3J_{H1\alpha\text{-}H2}$ (12.2 Hz) and $^3J_{H2\text{-}H3\alpha}$ (11.9 Hz) coupling constants and an NOE correlation between H-2 and Me-19 (Fig. 5). The ^1H NMR signal corresponding to H-6 was a broad *singlet*, indicating that H-6 and 6-OH occupy equatorial and axial positions, respectively. All other HMBC and NOESY correlations supported the overall structure and relative configuration of **9**, as shown in Figs. 4 and 5. The absolute configuration of **9** was determined by comparing the experimental ECD spectrum of **9** with that calculated by TDDFT method. The observed ECD spectrum ($\Delta\varepsilon_{204}$ –4.05, $\Delta\varepsilon_{224}$ +4.46) of **9** was in good agreement with that calculated for the 2*R*-configured model (Fig. 6). Consequently, the structure of **9** was established as shown in Fig. 3. The compound was named caesalsauterol.

Compound **10** was obtained as a colorless oil with an optical rotation, $[\alpha]_D$, of –15˚ (*c* 0.09, MeOH). Positive-ion HRESIFTMS revealed an $[M+Na]^+$ ion peak at *m/z* 441.1884 (calcd for $C_{23}H_{30}O_7Na^+$, 441.1884), consistent with the molecular formula $C_{23}H_{30}O_7$, which differs from that of compound **9** by 42 amu (C_2H_2O); this difference corresponds to the mass of an acetyl group. The NMR spectra were very similar to those

of compound **9**, except for the presence of additional signals at δ_H 2.04 (3H, s), δ_C 171.8 (CO), and δ_C 21.6 (CH_3), which supported the presence of an additional acetyl group in **10**. The significant downfield shift (+1.13 ppm) of H-6 in **10**, compared with the corresponding proton in **9**, indicated that the additional acetyloxy group is at C-6. The ^{1}H–^{1}H COSY correlations and HMBCs shown in Fig. 4 supported the proposed structure of **10**. The relative configuration of **10** was confirmed by analyzing the coupling constants and NOESY data (Fig. 5). The ^{1}H NMR spectrum of **10** exhibited a broad *singlet* for H-6, which indicates that H-6 and 6-AcO occupy equatorial and axial positions, respectively. The ECD spectrum of compound **10** exhibited a negative CE at 205 nm (Δε –3.97) and a positive CE at 224 nm (Δε +9.50), which were in good agreement with the CEs of compound **9**, indicating that the absolute configurations of both compounds are the same. Consequently, the structure of **10** was established as shown in Fig. 3. The compound was named 6-acetylcaesalsauterol.

Compound **11** was obtained as a colorless oil with an optical rotation, $[\alpha]_D$, of –5° (*c* 0.2, MeOH). Positive-ion HRESIFTMS exhibited an $[M+Na]^+$ ion peak at *m/z* 401.1568 (calcd for $C_{20}H_{26}O_7Na^+$, 401.1571), which is consistent with the molecular formula $C_{20}H_{26}O_7$. The NMR spectra of **11** were very similar to those of **9**, except for the lack of signals attributable to the exocyclic double bond and the appearance of a ketone carbonyl signal at δ_C 198.5 (C-14). The ^{1}H–^{1}H COSY correlations and HMBCs shown in Fig. 4 indicated that compound **11** is a 14-keto derivative of **9**. The relative configuration of **11** was confirmed by analyzing the coupling constants and NOESY data (Fig. 5). Because of their biogenetic relationships, the absolute configuration of **11** was considered to be the same as that of **9**. Consequently, the structure of **11** was established as shown in Fig. 3. The compound was named norcaesalsauterol.

Compounds **1**–**11** were evaluated for their larvicidal activities against the larvae of *Aedes albopictus*. Caesalacetal (**3**) and caesaljapin (**4**) isolated from the intact

seeds exhibited larvicidal activities with LC_{50} values of 3 and 9 μg/ml, respectively, while compounds **1**, **2**, and **5**–**11** were inactive.

As the hydroxylated diterpenoids **5**–**11** were not detected in the intact seeds of *C. decapetala*, **5**–**11** are postulated to be metabolic products of the seed constituents, caesaljaponin A (**1**), caesaljaponin B (**2**), caesalacetal (**3**), and caesaljapin (**4**), by the bruchid seed beetle *S. sauteri*. Possible metabolic pathways for **5**–**11** are suggested in Scheme 1. Caesaljapin (**4**) is possibly hydroxylated to afford 2-hydroxycaesaljapin (**6**), which in turn is further hydroxylated to yield 2,7-dihydroxycaesaljapin (**7**). Hydroxylation of the C-8 and C-14 positions of **6**, followed by lactonization between the 20-carboxyl and 8-hydroxyl groups should produce caesalsauteolide (**5**). It has been known that cytochrome P450 monooxygenases (P450s) of herbivorous insects mediate the hydroxylation of plant toxins to detoxify them (Scott et al., 1998; Schuler, 2011). It has also been reported that the methyl-substituted carbon center undergoes inversion of the configuration during the hydroxylation reaction by P450s (Jiang et al., 2006; Ortiz de Montellano, 2010). When P450s react with **6**, the abstraction of hydrogen at the C-14 position may occur to generate a radical intermediate. By binding of oxygen on the α-face of the radical intermediate, inversion of the configuration of C-14 could occur. Hydroxylation of the C-2 position of caesalacetal (**3**) affords 2-hydroxycaesalacetal (**8**), while dehydration of the 14-hydroxyl group and hydrolysis of the 20-acetyl group, as well as hydroxylation of the C-2 of caesaljaponin A (**1**) and/or caesaljaponin B (**2**), may afford 6-acetylcaesalsauterol (**10**), which, in turn is hydrolyzed to form caesalsauterol (**9**). Norcaesalsauterol (**11**) is thought to be produced by the oxidative cleavage of the exocyclic double bond between C-14 and C-17 of **9**.

3. Conclusions

Seven undescribed hydroxylated cassane-type furanoditerpenoids were isolated

from the pupal cases formed from the secretion/excretion products of the larvae of the wild bruchid seed beetle *Sulcobruchus sauteri* in infested seeds of *C. decapetala*. The structures of these compounds were elucidated by spectral interpretation. Although many furanoditerpenoids have been isolated from Fabaceae plants (Dickson et al., 2011; Maurya et al., 2012), 2-hydroxylated furanoditerpenoids are rare among them. Caesalacetal (**3**) and caesaljapin (**4**) that occur in these seeds exhibited larvicidal activities, while the hydroxylated furanoditerpenoids **5**–**11** obtained from the pupal cases were inactive. The hydroxylated furanoditerpenoids **5**–**11** were detected only in the pupal cases and were not present in the intact seeds of *C. decapetala*. These findings suggest that the larvae of the bruchid beetle *S. sauteri* detoxify larvicidal furanoditerpenoids, such as caesalacetal (**3**) and caesaljapin (**4**) that occur in the seeds of the host plant by regiospecific hydroxylation. The ability of the larvae of *S. sauteri* to hydroxylate these larvicidal constituents is believed to be one reason for the host-specificity of the bruchid beetle.

4. Experimental

4.1. General experimental procedures

Optical rotations were measured on a JASCO P-2200 polarimeter. IR spectra were recorded using a JASCO FT/IR-6300 spectrometer. UV spectra were obtained using a JASCO V-630 spectrometer. ECD spectra were measured using a JASCO J-725 spectropolarimeter. NMR spectra were acquired using a JEOL A400 spectrometer (400 MHz for ^{1}H, 100 MHz for ^{13}C). ^{1}H and ^{13}C NMR chemical shifts were referenced to residual solvent peaks: δ_H 3.30 (residual CHD_2OD) and δ_C 49.0 for CD_3OD. HRESIMS were carried out using a Thermo Fisher Scientific LTQ Orbitrap XL mass spectrometer at the Natural Science Center for Basic Research and Development (N-BARD), Hiroshima University. Column chromatography (CC) was performed using silica gel 60

(40 – 63 μm, Merck). Thin layer chromatography (TLC) was performed using pre-coated silica gel 60 F_{254} plates (Merck). High-performance liquid chromatography (HPLC)-photodiode array (PDA) analyses were performed with an Inertsil ODS-3 column (150 x 4.6 mm i.d., 5 μm) on a JASCO LC-2000 instrument equipped with a JASCO MD-2015 multiwavelength detector. The solvents, (A) CH_3CN and (B) 1% AcOH, were used as the mobile phase in the following gradient elution: 0–5 min, 60% A; 5–45 min, 60–80% A; 45–55 min 80–100% A with a flow rate of 0.6 ml/min.

4.2. Plant and insect materials

The seeds were collected from the tree of *Caesalpinia decapetala* (Roth) Alston (Leguminosae) which grows naturally on the river side (coordinates 34.5917° N, 132.7815° E) in Hiroshima Prefecture, Japan in November 2015 (dry season) and identified as described in the literature (Kamikawa et al., 2015, 2016b). The seeds were kept in plastic cases until adults of *Sulcobruchus sauteri* (Chrysomelidae, Bruchinae) emerged from infested seeds. Empty pupal cases were harvested after adult emergence. The seeds from which no adult has emerged were considered as intact seeds. Voucher specimens of the intact seed of *C. decapetala* (registry number HUM-PL-00004), the infested seed (registry number HUM-PL-00005), and *S. sauteri* (registry number HUM-Ins-0004264) have been deposited at the Hiroshima University Museum, Japan.

4.3. Extraction and isolation

The intact seeds (31 g) of *C. decapetala* were cut into small pieces and extracted with MeOH. The concentrated MeOH extract was subjected to ODS CC eluted with MeOH–H_2O (0:100 to 100:0) to yield nine fractions A to I. Fraction F (MeOH–H_2O, 6:4) (12 mg) was purified by silica gel CC with acetone–hexane (0:100 to 100:0) to afford caesaljaponin B (**2**) (6 mg). Fraction G (MeOH–H_2O, 7:3) (13 mg) was

purified by silica gel CC with acetone–hexane (0:100 to 100:0) to afford caesaljaponin A (**1**) (4 mg). Fraction H (MeOH–H_2O, 8:2) (77 mg) was purified by silica gel CC with acetone–hexane (0:100 to 100:0) to afford caesalacetal (**3**) (4 mg), and caesaljapin (**4**) (13 mg).

The pupal cases (4.5 g) extracted with MeOH (50 ml) at room temperature for 2 days. The concentrated MeOH extract (518 mg), after being suspended with H_2O, was sequentially partitioned with hexane and EtOAc. The EtOAc-soluble portion (406 mg) was subjected to ODS CC eluted with MeOH–H_2O (0:100 to 100:0) to yield eleven fractions J to T. Fraction K (MeOH–H_2O, 1:19) (4 mg) was purified by ODS CC with CH_3CN–H_2O (0:100 to 100:0) to afford **11** (1 mg). Fraction L (MeOH–H_2O, 1:9) (4 mg) was purified by ODS CC with CH_3CN–H_2O (0:100 to 100:0) to afford **7** (2 mg). Fraction M (MeOH–H_2O, 1:4) (5 mg) was purified by ODS CC with CH_3CN–H_2O (0:100 to 100:0) to afford **5** (2 mg). Fraction N (MeOH–H_2O, 3:7) (5 mg) was purified by silica gel CC with acetone–hexane (0:100 to 100:0) to afford **9** (2 mg). Fraction O (MeOH–H_2O, 2:3) (20 mg) was purified by silica gel CC with acetone–hexane (0:100 to 100:0) to afford **8** (3 mg) and **10** (6 mg). Fraction P (MeOH–H_2O, 1:1) (3 mg) was purified by ODS CC with CH_3CN–H_2O (0:100 to 100:0) to afford **6** (1 mg).

*4.4. Caesalsauteolide (**5**)*

Colorless oil; $[\alpha]_D^{25}$ –28° (*c* 0.04, MeOH); UV (CH_3CN) λ_{max} (log ε) 200 (4.01), 216 (4.02) nm; ECD (CH_3CN) λ_{max} (Δε) 190 (+2.01), 216 (–2.86), 247 (+0.42); IR (film) ν_{max} 3396, 1760, 1724, 1507, 1456 cm^{-1}; ^1H NMR, see Table 1; ^{13}C NMR, see Table 2; (+)HRESIFTMS *m/z* 413.1570 $[M+Na]^+$ (calcd for $C_{21}H_{26}O_7Na^+$, 413.1571).

*4.5. 2-Hydroxycaesaljapin (**6**)*

Colorless oil; $[\alpha]_D^{25}$ +8˚ (*c* 0.1, MeOH); UV (MeOH) λ_{max} (log ε) 217 (3.93) nm; ECD (MeOH) λ_{max} (Δε) 216 (+2.67); IR (film) ν_{max} 3700–2800, 1723, 1650, 1507, 1456 cm^{-1}; ^1H NMR, see Table 1; ^{13}C NMR, see Table 2; (–)HRESIFTMS *m/z* 375.1817 $[M–H]^-$ (calcd for $C_{21}H_{27}O_6^-$, 375.1813).

*4.6. 2,7-Dihydroxycaesaljapin (**7**)*

Colorless oil; $[\alpha]_D^{25}$ +3˚ (*c* 0.2, MeOH); UV (MeOH) λ_{max} (log ε) 217 (4.11) nm; ECD (MeOH) λ_{max} (Δε) 215 (+2.60); IR (film) ν_{max} 3700–2800, 1715, 1652, 1507, 1456 cm^{-1}; ^1H NMR, see Table 1; ^{13}C NMR, see Table 2; (+)HRESIFTMS *m/z* 391.1765 $[M–H]^-$ (calcd for $C_{21}H_{27}O_7^-$, 391.1762).

*4.7. 2-Hydroxycaesalacetal (**8**)*

Colorless oil; $[\alpha]_D^{25}$ +19˚ (*c* 0.004, MeOH); UV (MeOH) λ_{max} (log ε) 214 (3.72) nm; ECD (MeOH) λ_{max} (Δε) 219 (+1.72); IR (film) ν_{max} 3391, 1723, 1646, 1506, 1456 cm^{-1}; ^1H NMR, see Table 1; ^{13}C NMR, see Table 2; (+)HRESIFTMS *m/z* 399.1778 $[M+Na]^+$ (calcd for $C_{21}H_{28}O_6Na^+$, 399.1778).

*4.8. Caesalsauterol (**9**)*

Colorless oil; $[\alpha]_D^{25}$ –6˚ (*c* 0.2, MeOH); UV (CH_3CN) λ_{max} (log ε) 209 (3.99), 232 (3.93) nm; ECD (CH_3CN) λ_{max} (Δε) 204 (–4.05), 224 (+4.46); IR (film) ν_{max} 3392, 1716, 1651, 1507, 1457 cm^{-1}; ^1H NMR, see Table 1; ^{13}C NMR, see Table 2; (+)HRESIFTMS *m/z* 399.1779 $[M+Na]^+$ (calcd for $C_{21}H_{28}O_6Na^+$, 399.1778).

*4.9. 6-Acetylcaesalsauterol (**10**)*

Colorless oil; $[\alpha]_D^{25}$ –15˚ (*c* 0.09, MeOH); UV (MeOH) λ_{max} (log ε) 210 (4.02), 245sh (3.96) nm; ECD (MeOH) λ_{max} (Δε) 205 (–3.97), 224 (+9.50); IR (film) ν_{max} 3418,

1731, 1715, 1652, 1508, 1456 cm^{-1}; ^{1}H NMR, see Table 1; ^{13}C NMR, see Table 2; (+)HRESIFTMS *m/z* 441.1884 $[M+Na]^+$ (calcd for $C_{23}H_{30}O_7Na^+$, 441.1884).

*4.10. Norcaesalsauterol (**11**)*

Colorless oil; $[\alpha]_D^{25}$ –5° (*c* 0.2, MeOH); UV (CH_3CN) λ_{max} (log ε) 198 (4.43), 217sh (3.97), 256 (3.84) nm; ECD (CH_3CN) λ_{max} (Δε) 202 (+11.01), 260 (–5.43), 306 (+3.01); IR (film) ν_{max} 3300, 1717, 1660, 1570, 1515, 1456 cm^{-1}; ^{1}H NMR, see Table 1; ^{13}C NMR, see Table 2; (+)HRESIFTMS *m/z* 401.1568 $[M+Na]^+$ (calcd for $C_{20}H_{26}O_7Na^+$, 401.1571).

4.11. ECD calculation

Theoretical ECD spectra were predicted from a standard calculation procedure (Bringmann et al., 2009) as follows: Conformational searches of **5** and **9** were performed with CONFLEX8 (Goto and Osawa, 1989, 1993; Goto et al., 2017) with MMFF94S (2010-12-04HG) as the force field on a commercially available PC (operating system: Windows 10 Pro for Workstations, CPU: Intel Xeon E5-1650 v4 processor 3.60 GHz, RAM 32 GB). Appropriate conformers (population >1%) were further optimized with Gaussian09 software (Frisch et al., 2013) at the approximation level of B3LYP/6-31G(d) supposing no solvent on a PC (Operating System: CentOS a Linux, CPU: 12 Intel Xeon E5-2643 v3 processors 3.40 GHz, RAM 32 GB). The population of the obtained conformers were analysed by considering their Boltzmann distribution at 298 K based on their internal and vibrational energies. The dominant conformers (total population >90%) were subjected to time-dependent simulations with the basis set cc-pVDZ with the hybrid functional B3LYP supposing no solvent. For each conformer, the resultant rotational strengths were converted into Gaussian curves (bandwidth sigma = 3000 cm^{-1}) and correctively summed to give the ECD spectrum.

4.12. Larvicidal assay

Larvicidal activities were evaluated using a modification of the method reported by Meepagala et al. (2016). Five first instar larvae of *Aedes albopictus*, in deionized water (198 µl), were transferred the following day into 96-well plates. Isolated compounds were dissolved in MeOH and serially diluted to the required concentrations with MeOH. A 2-µl aliquot of the diluted sample solution in MeOH was added to each well with gently mixing. Larval mortalities were assessed 24 h after treatment. Larvae that exhibited no movement after agitation of the water with a pipet tip were deemed to be dead. Permethrin was used as a positive control (LC_{50} = 0.0005 µg/ml), while deionized was the negative control. All experiments were performed in duplicate.

Acknowledgments

This work was supported in part by JSPS KAKENHI Grant Number 18K05335. We thank Editage (http://www.editage.jp) for English language editing.

References

Bringmann, G., Bruhn, T., Maksimenka, K., Hemberger, Y., 2009. The assignment of absolute stereostructures through quantum chemical circular dichroism calculations. Eur. J. Org. Chem. 2009, 2717–2727.

Dickson, R.A., Fleischer, T.C., Houghton, P.J., 2011. Cassane-type diterpenoids from the genus *Caesalpinia*. Pharmacog. Commun. 1, 63–77.

Frisch, M.J., Trucks, G.W., Schlegel, H.B., Scuseria, G.E., Robb, M.A., Cheeseman, J.R., Scalmani, G., Barone, V., Mennucci, B., Petersson, G.A., Nakatsuji, H., Caricato, M., Li, X., Hratchian, H.P., Izmaylov, A.F., Bloino, J., Zheng, G.,

Sonnenberg, J.L., Hada, M., Ehara, M., Toyota, K., Fukuda, R., Hasegawa, J., Ishida, M., Nakajima, T., Honda, Y., Kitao, O., Nakai, H., Vreven, T., Montgomery, Jr., J.A., Peralta, J.E., Ogliaro, F., Bearpark, M., Heyd, J.J., Brothers, E., Kudin, K.N., Staroverov, V.N., Keith, T., Kobayashi, R., Normand, J., Raghavachari, K., Rendell, A., Burant, J.C., Iyengar, S.S., Tomasi, J., Cossi, M., Rega, N., Millam, J.M., Klene, M., Knox, J.E., Cross, J.B., Bakken, V., Adamo, C., Jaramillo, J., Gomperts, R., Stratmann, R.E., Yazyev, O., Austin, A.J., Cammi, R., Pomelli, C., Ochterski, J.W., Martin, R.L., Morokuma, K., Zakrzewski, V.G., Voth, G.A., Salvador, P., Dannenberg, J.J., Dapprich, S., Daniels, A.D., Farkas, O., Foresman, J.B., Ortiz, J.V., Cioslowski, J., Fox, D.J., 2013. Gaussian 09, Revision D.01. Gaussian Inc., Wallingford CT.

Goto, H., Osawa, E., 1989. Corner flapping: a simple and fast algorithm for exhaustive generation of ring conformations. J. Am. Chem. Soc. 111, 8950–8951.

Goto, H., Osawa, E., 1993. An efficient algorithm for searching low-energy conformers of cyclic and acyclic molecules. J. Chem. Soc., Perkin Trans. 2, 187–198.

Goto, H., Obata, S., Nakayama, N., Ohta, K., 2017. CONFLEX 8. CONFLEX Corporation, Tokyo, Japan.

Jiang, R.-W., Ma, S.-C., He, Z.-D., Huang, X.-S., But, P.P.-H., Wang, H., Chan, S.-P., Ooi, V.E.-C., Xu, H.-X., Mak, T.C.W., 2002. Molecular structures and antiviral activities of naturally occurring and modified cassane furanoditerpenoids and friedelane triterpenoids from *Caesalpinia minax*. Bioorg. Med. Chem. 10, 2161–2170.

Jiang, Y., He, X., He, Z.-D., Ortiz de Montellano, P.R., 2006. Radical intermediates in the catalytic oxidation of hydrocarbons by bacterial and human cytochrome P450 enzymes. Biochemistry 45, 533–542.

Kamikawa, S., Ohta, E., Ohta, S., 2015. Caesaljaponins A and B: New cassane-type furanoditerpenoids from the seeds of *Caesalpinia decapetala* var. *japonica*. Helv. Chim. Acta 98, 336–342.

Kamikawa, S., Oshimo, S., Ohta, E., Nehira, T., Ômura, H., Ohta, S., 2016a. Cassane diterpenoids from the roots of *Caesalpinia decapetala* var. *japonica* and structure revision of caesaljapin. Phytochemistry 121, 50–57.

Kamikawa, S., Ohta, E., Nehira, T., Ômura, H., Ohta, S., 2016b. Structure revision of caesalpinistas A and B and isolation of a new furanoditerpenoid from the cotyledons of *Caesalpinia decapetala* var. *japonica*. Helv. Chim. Acta 99, 133–137.

Maurya, R., Ravi, M., Singh, S., Yadav, P.P., 2012. A review on cassane and norcassane diterpenes and their pharmacological studies. Fitoterapia 83, 272–280.

Meepagala, K.M., Estep, A.S., Becnel, J.J., 2016. Larvicidal and adulticidal activity of chroman and chromene analogues against susceptible and permethrin-resistant mosquito strains. J. Agric. Food. Chem. 64, 4914–4920.

Namikoshi, M., Nakata, H., Nuno, M., Ozawa, T., Saitoh, T., 1987. Homoisoflavonoids and related compounds. III. Phenolic constituents of *Caesalpinia japonica* Sieb. *et* Zucc. Chem. Pharm. Bull. 35, 3568–3575.

Ochieng, C.O., Owuor, P.O., Manguro, L.A.O., Akala, H., Ishola, I.O., 2012. Antinociceptive and antiplasmodial activities of cassane furanoditerpenes from *Caesalpinia Volkensii* H. root bark. Fitoterapia 83, 74–80.

Ogawa, K., Aoki, I., Sashida, Y., 1992. Caesaljapin, a cassane diterpenoid from *Caesalpinia decapetala* var. *japonica*. Phytochemistry 31, 2897–2898.

Ortiz de Montellano, P.R., 2010. Hydrocarbons hydroxylation by cytochrome P450 enzymes. Chem. Rev. 110, 932–948.

Schuler, M.A., 2011. P450s in plant–insect interactions. Biochim. Biophys. Acta 1814,

36–45.

Scott, J.G., Liu, N., Wen, Z., 1998. Insect cytochromes P450: diversity, insecticide resistance and to plant toxins. Comp. Biochem. Physiol. 121, 147–155.

Yang, Z.-Y., Yin, Y.-H., Hu, L.-H., 2009. Five new cassane-type diterpenes from *Caesalpinia crista*. Helv. Chim. Acta 92, 121–126.

Watanabe, N., 1985. Oviposition habit of *Sulcobruchus sauteri* (Pic) and its significance in speculation on the pre-agricultural life of seed beetles attacking stored pulses (Coleoptera, Bruchidae). Kontyu 53, 391–397.

Wu, J., Chen, G., Xu, X., Huo, X., Wu, S., Wu, Z., Gao, H., 2014. Seven new cassane furanoditerpenes from the seeds of *Caesalpinia minax*. Fitoterapia 92, 168–176.

Table 1
^{1}H NMR spectroscopic data (δ_H, mult (*J* in Hz)) for **5**–**11** in CD_3OD (400 MHz)

No	**5**	**6**	**7**	**8**	**9**	**10**	**11**
1α	1.34 (t, 11.9)	0.91 (t, 11.7)	0.78 (t, 11.6)	1.11 (dd, 12.8, 11.0)	1.00 (t, 12.2)	0.83 (t, 11.9)	1.03 (t, 11.9)
1β	2.26 (dd, 11.9, 4.0)	2.75 (dd, 11.7, 3.4)	2.71 (m)	2.13 (dd, 12.8, 4.6)	2.27 (br d, 12.2)	2.87 (br d, 11.9)	2.31 (br d, 11.9)
2	4.22 (tt, 11.9, 4.0)	4.19 (m)	4.31 (m)	4.21 (dddd, 12.2, 11.0, 4.6, 4.3)	3.81 (m)	3.97 (tt, 11.9, 4.0)	3.85 (tt, 11.9, 3.7)
3α	1.60 (t, 11.9)	1.71 (t, 12.2)	1.68 (t, 11.9)	1.41 (t, 12.2)	1.68 (t, 11.9)	1.69 (t, 11.9)	1.70 (t, 11.9)
3β	1.93 (br d, 11.9)	1.82 (dd, 12.2, 4.9)	1.81 (br d, 11.9)	1.97 (dd, 12.2, 4.3)	1.84 (br d, 11.9)	1.86 (ddd, 11.9, 4.0, 2.1)	1.84 (br d, 11.9)
5	2.30 (dd, 13.1, 4.6)	1.89 (dd, 12.7, 3.4)	1.82 (dd, 12.5, 2.1)	1.81 (br s)	2.04 (br s)	2.12 (br s)	2.04 (br s)
6α	1.74 (dq, 13.1, 4.6)	1.08 (br d, 12.7)	1.29 (m)	4.51 (br d, 4.3)	3.90 (br s)	5.03 (br s)	3.90 (br s)
6β	1.51 (qd, 13.1, 4.3)	2.35 (qd, 12.7, 3.4)	2.68 (ddd, 12.5, 11.6, 10.7)				
7α	1.96 (td, 13.1, 4.6)	1.44 (tdd, 12.7, 10.7, 4.9)	3.51 (td, 10.7, 4.9)	1.78 (dd, 11.9, 5.8)	1.53 (br dd, 14.0, 11.9)	1.52 (br dd, 14.6, 12.5, 2.7)	1.45 (ddd, 14.6, 12.5, 3.1)
7β	2.27 (m)	1.70 (m)		1.57 (t, 11.9)	2.31 (br d, 14.0)	2.39 (ddd, 15.0, 4.6, 3.1)	2.40 (ddd, 14.6, 4.3, 3.7)
8		2.25 (m)	2.36 (ddd, 11.6, 10.7, 4.6)	1.89 (ddd, 11.9, 9.8, 4.6)	2.95 (br t, 11.9)	2.53 (br t, 12.5)	3.16 (td, 12.5, 4.3)
9	2.58 (dd, 8.5, 7.9)	1.70 (m)	1.58 (m)	1.85 (m)	1.50 (m)	1.69 (m)	1.98 (dt, 12.5, 8.5)
11α	2.84 (dd, 17.1, 7.9)	2.77 (dd, 16.6, 6.2)	2.75 (dd, 16.5, 5.8)	2.69 (dd, 16.5, 5.5)	2.85 (d, 8.2)	2.87 (dd, 16.8, 5.5)	3.09 (d, 8.5)
11β	2.41 (dd, 17.1, 8.5)	2.19 (dd, 16.6, 10.9)	2.30 (dd, 16.5, 11.3)	2.32 (dd, 16.5, 10.7)	2.85 (d, 8.2)	2.95 (dd, 16.8, 11.0)	3.09 (d, 8.5)
14		2.59 (qd, 7.3, 4.6)	3.04 (qd, 7.0, 4.6)	2.63 (dq, 7.0, 4.6)			
15	6.46 (d, 1.8)	6.17 (d, 1.8)	6.17 (d, 1.8)	6.20 (d, 1.8)	6.47 (d, 1.8)	6.47 (d, 1.8)	6.62 (d, 2.1)
16	7.36 (d, 1.8)	7.21 (d, 1.8)	7.19 (d, 1.8)	7.25 (d, 1.8)	7.28 (d, 1.8)	7.27 (d, 1.8)	7.48 (d, 2.1)
17a	1.48 (s)	0.98 (d, 7.3)	1.03 (d, 7.0)	1.02 (d, 7.0)	5.05 (d, 2.1)	5.10 (d, 2.1)	
17b					4.78 (d, 2.1)	4.77 (d, 2.1)	
19	1.22 (s)	1.12 (s)	1.19 (s)	1.47 (s)	1.61 (s)	1.39 (s)	1.60 (s)
20a				5.22 (br s)	4.12 (d, 12.8)	4.14 (d, 12.8)	4.18 (d, 12.8)
20b					3.78 (d, 12.8)	4.01 (d, 12.8)	3.85 (d, 12.8)
21	3.70 (s)	3.68 (s)	3.68 (s)	3.68 (s)	3.71 (s)	3.70 (s)	3.70 (s)
OAc						2.04 (s)	

Table 2

^{13}C NMR spectroscopic data (δ_C) for **5**–**11** in CD_3OD (100 MHz)

No	**5**	**6**	**7**	**8**	**9**	**10**	**11**
1	37.6	46.0	46.9	38.7	47.8	43.6	46.6
2	63.8	65.2	65.6	65.6	64.4	64.7	64.3
3	46.0	46.1	46.3	43.5	47.7	47.5	47.8
4	49.9	49.9	49.7	46.0	50.4	49.9	50.3
5	44.8	51.2	48.2	55.2	52.0	50.4	52.1
6	23.8	24.0	33.3	78.8	68.4	72.1	68.1
7	29.9	31.4	72.3	37.2	40.2	36.3	37.1
8	88.5	36.8	44.2	38.3	35.1	33.7	43.9
9	52.3	44.9	44.1	46.5	53.8	53.7	53.9
10	55.0	49.9	49.8	51.0	44.4	45.2	44.6
11	21.8	25.2	25.5	25.9	23.9	24.9	24.5
12	148.6	149.5	150.1	149.7	153.4	153.7	169.3
13	122.4	123.9	123.3	124.4	120.1	119.7	120.7
14	70.1	32.7	28.4	31.2	144.2	143.3	198.5
15	109.1	110.5	110.6	110.6	107.3	107.2	107.1
16	143.1	141.8	141.6	142.1	142.7	142.7	144.7
17	22.7	17.4	16.9	17.2	103.7	104.4	
18	178.5	179.2	179.5	180.4	179.7	179.1	179.5
19	16.8	16.9	17.1	19.6	20.0	19.9	20.0
20	180.5	178.3	179.6	100.2	64.5	61.2	64.2
21	52.9	52.6	52.6	52.6	52.9	52.9	52.9
OAc						171.8	
						21.6	

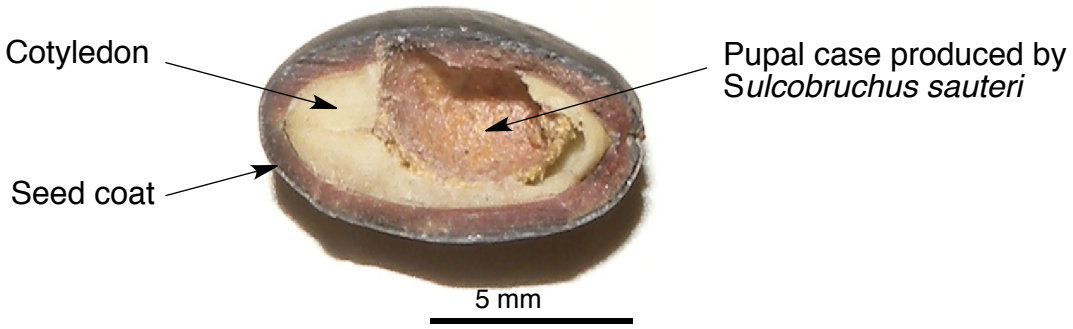

Fig. 1. Cross-section of an infested seed of *C. decapetala*.

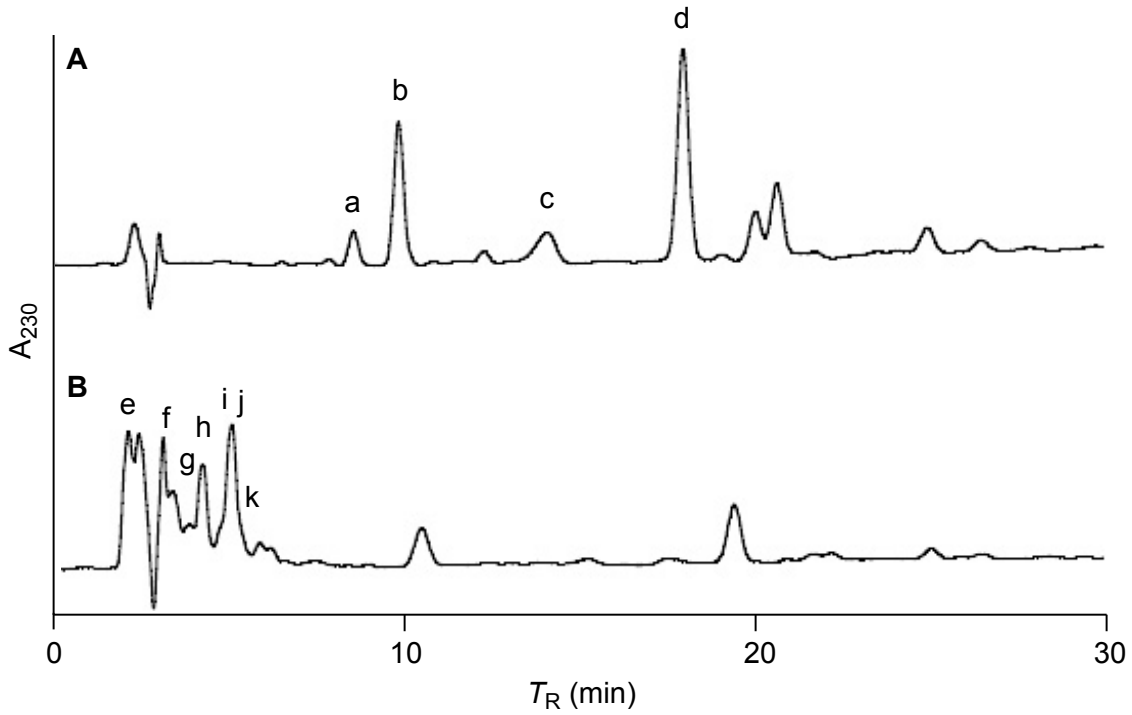

Fig. 2. Representative HPLC-PDA profiles of the EtOAc-soluble fractions of: (A) the intact seeds of *C. decapetala* and (B) the pupal cases produced by *S. sauteri.* Detection was performed at 230 nm. a, caesaljaponin B (**2**); b, caesaljaponin A (**1**); c, caesalacetal (**3**); d, caesaljapin (**4**); e, norcaesalsauterol (**11**); f, 2,7-dihydroxycaesaljapin (**7**); g, caesalsauteolide (**5**); h, caesalsauterol (**9**); i, 2-hydroxycaesalacetal (**8**); j, 6-acetylcaesalsauterol (**10**); k, 2-hydroxycaesaljapin (**6**).

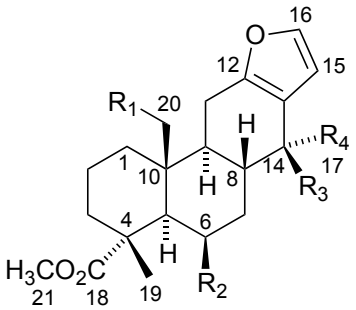

1: $R_1 = R_2 = OAc$, $R_3 = OH$, $R_4 = Me$
2: $R_1 = R_2 = OAc$, $R_3 = Me$, $R_4 = OH$
12: $R_1 = R_2 = OH$, $R_3 = H$, $R_4 = Me$

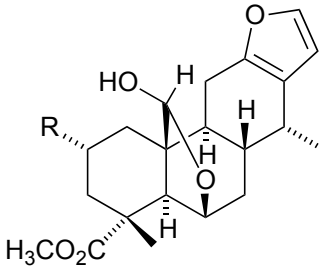

3: R = H
8: R = OH

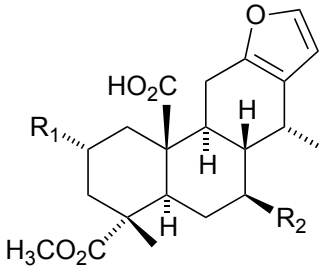

4: $R_1 = R_2 = H$
6: $R_1 = OH$, $R_2 = H$
7: $R_1 = R_2 = OH$

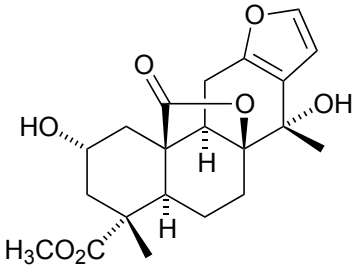

5

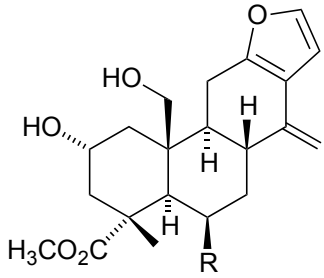

9: R = OH
10: R = OAc

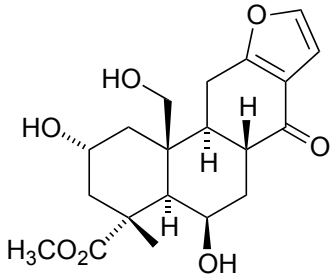

11

Fig. 3. The structures of compounds **1**–**12**.

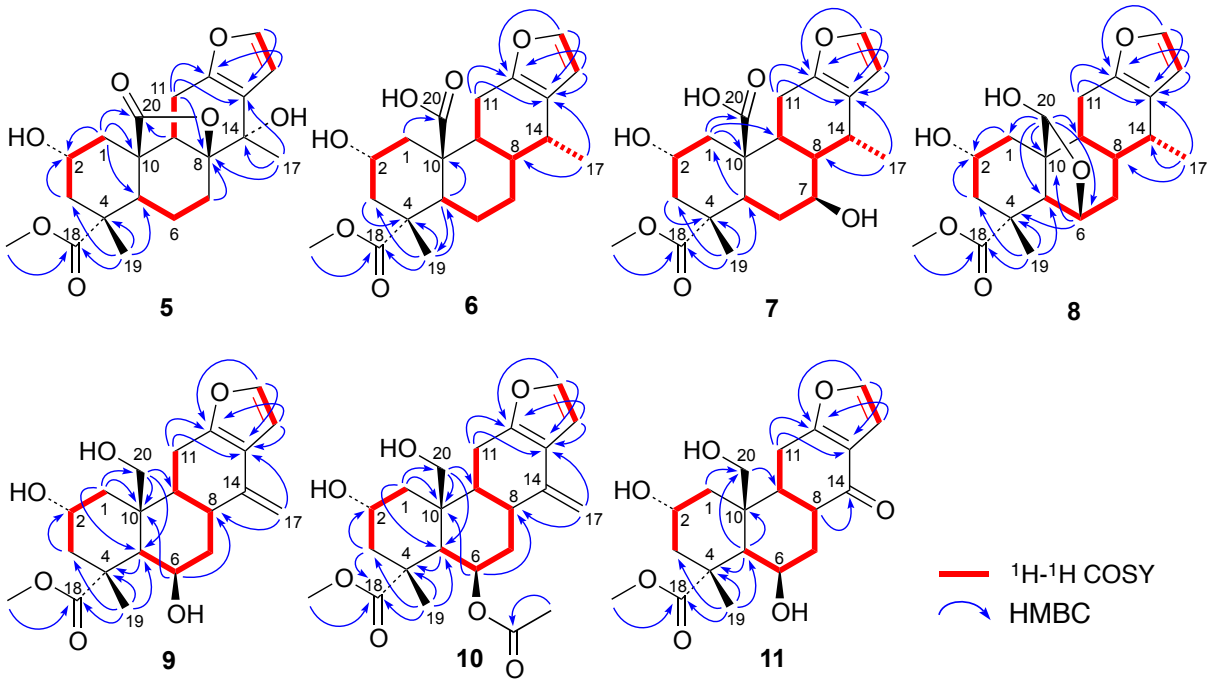

Fig. 4. ^{1}H–^{1}H COSY and key HMBC correlations for compounds **5**–**11**.

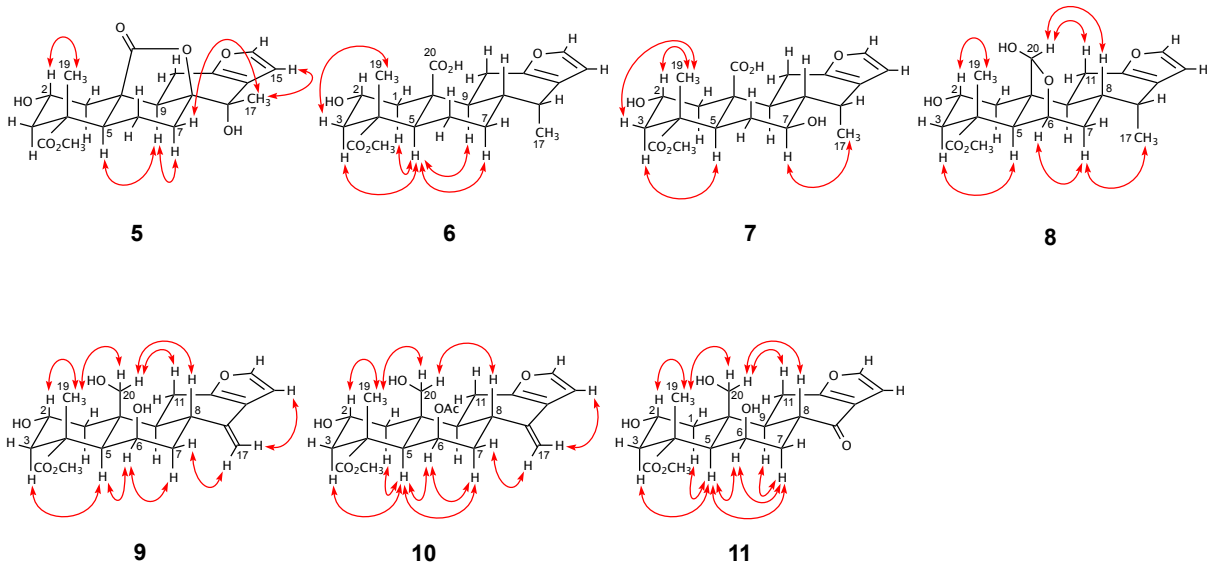

Fig. 5. Key NOEs for compounds **5**–**11**.

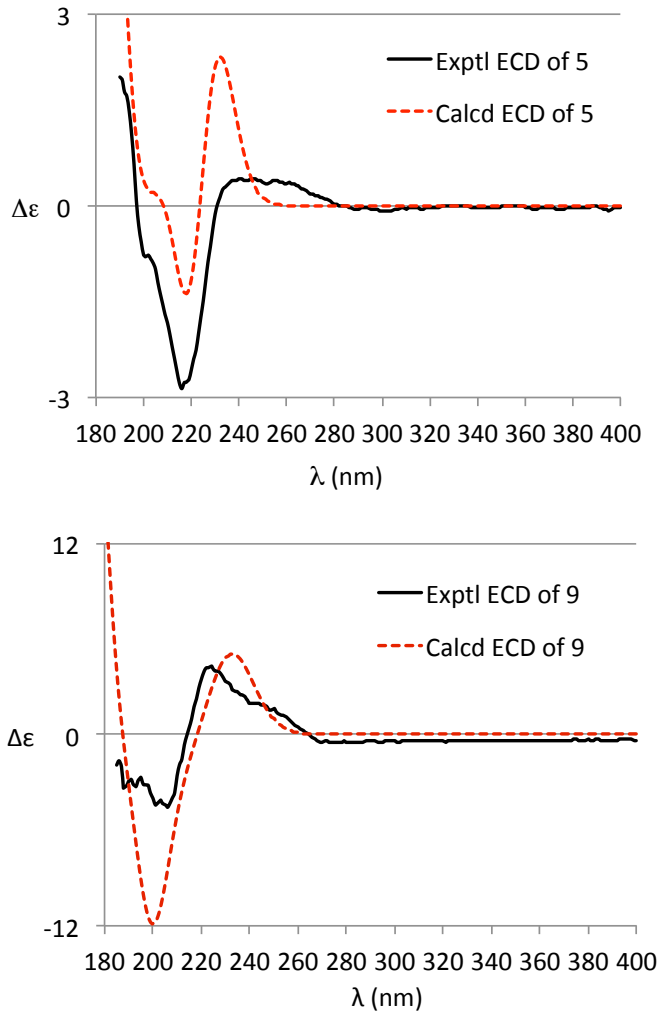

Fig. 6. Experimental (solid lines) and calculated (dashed lines) ECD spectra of **5** and **9**.

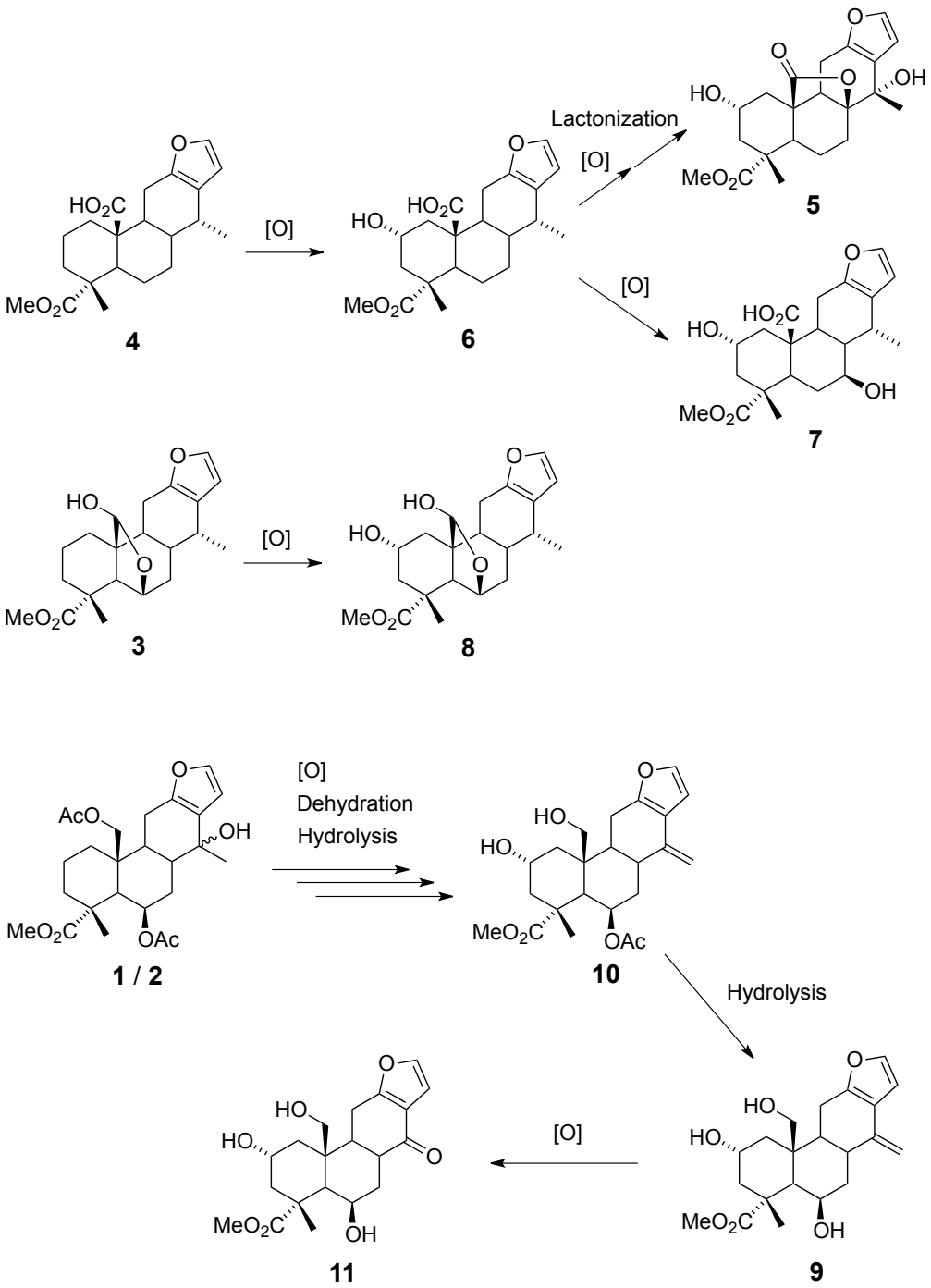

Scheme 1. Possible metabolic pathways from the constituents **1**–**4** of the seeds of *C. decapetala* to compounds **5**–**11** by *S. sauteri*.